Use of Novel Spudcan Shapes for Mitigating Punch-Through Hazards

J.M. Lee, Y.H. Kim, M.S. Hossain*, M.J. Cassidy and Y. Hu
Centre for Offshore Foundation Systems
THE UNIVERSITY OF WESTERN AUSTRALIA

J.H. Won, J.S. Park and M.J. Jun
DAEWOO SHIPBUILDING & MARINE ENGINEERING CO. LTD., KOREA
** Corresponding author: muhammad.hossain@uwa.edu.au*

ABSTRACT
Jack-up geotechnical hazards such as punch-through failures (i.e. unpredicted and rapid leg penetration) continue to occur despite the jack-up industry efforts to minimise these risks. Punch-through incidents occur in stratified soil conditions with a surface or interbedded strong (sand or stiff clay/silt) layer gets pushed into an underlying weak layer. Improvements have been made on jack-up installation guidelines and site specific assessment as documented in the recently finalised version of ISO guidelines 19905-1 [1] and the completed joint industry project 'InSafeJIP [2]'. Recently, improved design approaches have been developed for predicting penetration depth of conventional spudcans in stratified soils. Once the risk of punch-through failure is identified at a site, mitigation methods are required to allow a safer installation of the rig. This paper reports preliminary results of 1g model tests and large deformation finite element (LDFE) analyses (using the Coupled Eulerian-Lagrangian, CEL, approach in the commercial finite element package ABAQUS) undertaken on two novel spudcan shapes – one with a peripheral skirt and four evenly spaced slots close to the skirt, and the other featuring six evenly spaced holes with slopes at the base. The aim is to investigate if the spudcan shape itself can be used to mitigate potential punch-through when compared to a conventional spudcan. It is found that the novel spudcans may be an effective measure at mitigating the risk of punch-through failure. More extensive investigations are being carried out through centrifuge model tests and LDFE analyses using the RITSS (remeshing and interpolation technique with small strain) approach in ABAQUS.

KEYWORDS: jack-up; novel spudcan shape; punch-through; 1g test; large deformation finite element analysis

INTRODUCTION
Mobile jack-up rigs are used widely in the offshore oil and gas industry for installing new platforms, maintenance work and drilling and even for production for small, marginal fields. There has been continual evolution of rig operations into new regions and greater water depths, and today independent-legged jack-up rigs are used for most offshore drilling operations in water depths up to around 150 m. Typically this type of rig consists of a buoyant triangular platform supported by three independent vertically retractable *K*-lattice legs, each resting on a spudcan. Spudcans are typically 10 to 20 m (equivalent area) diameter and generally saucer-shaped polygonal or quasi-circular foundation. Alternative shapes, such as the use of external skirts, have been considered by the offshore industry due to their potential to increase footing resistance capacity under storm loading conditions. However, they are not commonly used due to the concerns of the potential difficulties during installation and preloading processes.

Jack-ups have a self-installation capacity. When on site their legs are lowered to the seabed and the footings are then pre-loaded by pumping sea-water into ballast tanks in the hull. This is to ensure that the footings have sufficient reserve capacity in any extreme storm design event.

For the jack-up industry, spudcan punch-through failure (i.e. unexpected rapid penetration of the footings in layered soil profiles) in layered soils is one of the major concerns related to geotechnical/structural failures during this installation and preloading process. Punch-through incidents can occur in stratified soil conditions with a surface or interbedded strong (sand or stiff clay/silt) layer overlying a weak layer. Excessive uncontrolled rapid leg plunge can lead to buckling of the leg, effectively decommissioning the platform, or even toppling of the jack-up unit (Aust [3]; Kostelnik et al. [4]). Although the potential hazard of crustal features is well

documented (SNAME [5]), jack-ups continue to suffer failures, causing economic loss of $5~50 million per incident (Jack et al. [6, 7]). Two recent examples are the failures of the Noble David Tinsley in May 2009 off the coast of Qatar, and the Noble Kenneth Delaney in 2012 offshore India (Jack et al. [7]).

Once the risk of punch-through failure is identified at a site, mitigation methods are required to allow a safer installation of the rig. Traditionally, installation procedures (such as leg by leg preloading instead of simulatneous preloading, preloading with the hul at the water surface i.e. with zero or negetive airgap rather than positive air gap; InSafeJIP [2]) have been used for easing punch-through or controlling leg penetration. Recently, several other mitigation methods have been discussed (InSafeJIP [2]); notably (a) degrading the strong layer by cyclically loading the spudcan (Erbrich [8]); (b) perforation drilling (Brennan et al. [9]; Hossain et al. [10, 11]; InSafeJIP [2]); and (c) using a jack-up with skirted foundations/spudcans (Svanø & Tjelta [12]; Gan et al. [13]; Hossain et al. [14]). The former two methods require separate expensive operations to be carried out. Although these methods have been trialled and used in practice, there is no systematic study and guidance on the optimum selection of these measures and thus are not suggested in the ISO standard.

The overarching aim of this research is to provide guidance on mitigating punch-through failures during jack-up installation by adjusting the footing design. The alternative footing shapes to be investigated are shown in Figures 1b and 1c, where the supudcan has modified underside shape, evenly spaced slots (spudcan S) or slopes and holes (spudcan H) at the spudcan base and a skirt along the periphery of the spudcan. The notion is to force the confroted soil to flow through the spudcan.

This paper reports the preliminary results from an investigation through 1g model tests (sand-over-clay) and large-deformation finite element analyses (stiff-over-soft clay). A parametric investigation was undertaken, varying the relevant range of various parameters related to the novel spudcans' geometry, soil strength and strong layer's thickness. The main objective of this study is to investigate if the spudcan shape itself can be used to mitigate the potential punch-through failure with a conventional spudcan.

1G MODEL TEST

Experimental program

The experimental programme comprised 1g modelling of vertical penetration of spudcans in sand-over-clay. The work was carried out in the 1g test facility at the University of Western Australia. The soil sample was prepared in a standard rectangular 'strongbox', which has internal dimensions of 650 (length) × 390 (width) × 325 (depth) mm. A layer of free water was maintained at the sample surface.

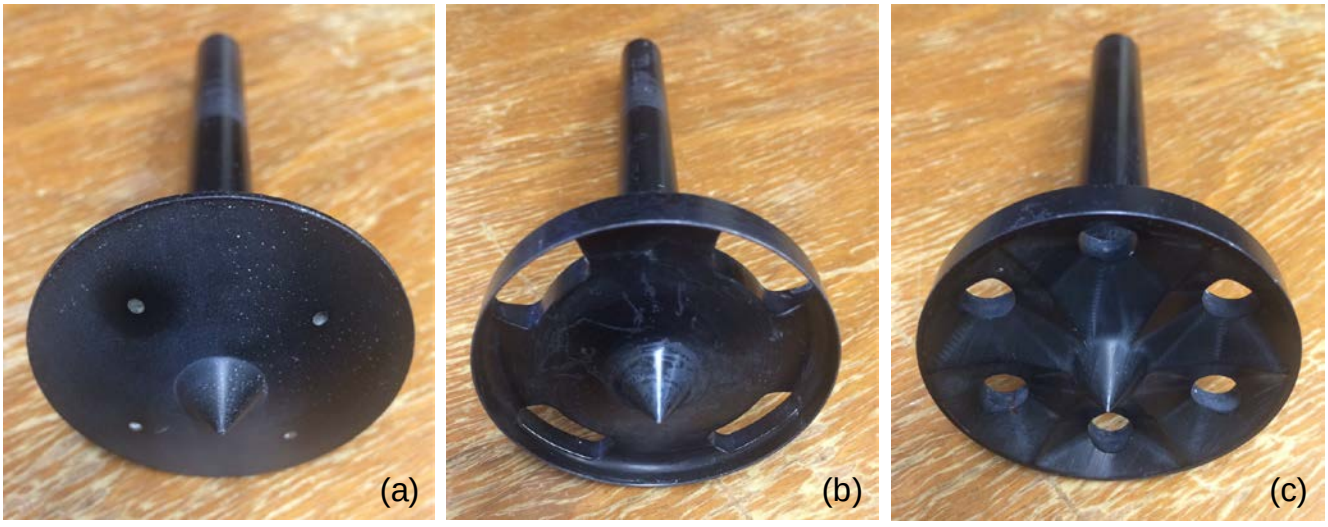

FIGURE 1. Shapes of model spudcans used in 1g tests (diameter, D = 60 mm): (a) Conventional (spudcan A); (b) 4-slot (spudcan S); (c) 6-hole (spudcan H)

Model tests were performed using a conventional spudcan (spudcan A) and two novel spudcans (spudcan S and spudcan H) of 60 mm diameter. The shape of spudcan A (Figure 1a) was chosen similar to the spudcans of the 'Marathon LeTourneau Design, Class 82-SDC' jack-up rig, as illustrated by Menzies & Roper [15]. The basic shape of spudcan S (Figure 1b) is similar to spudcan A. A skirt of height 8 mm was added around the periphery, and four evenly spaced slots (8 mm × ~19.8 mm) were made at the base close to the skirt. The ratios of skirt length to diameter (L/D) was 0.13. The shape of spudcan H (Figure 1c) is innovative featuring six evenly spaced holes (of diameter d_h = 8.42 mm) with slopes at the base. A total of six spudcan penetration tests were performed, which are summarised in Table 1. A load cell fitted between the loading arm of the actuator and the foundation shaft measured load-penetration responses in this displacement controlled system.

Preparation of sample

Super fine silica sand and kaolin clay were used to produce layered soil profiles. The super fine silica sand has its properties of specific gravity, G_s = 2.65; average particle size, d_{50} = 0.190; maximum void ratio, e_{max} = 0.747; minimum void ratio, e_{min} = 0.449; critical state friction angle, ϕ_{cv} = 32°; and the kaolin clay has its properties of G_s = 2.6; liquid limit, LL = 61%; plasticity index, I_p = 34; consolidation coefficient, c_v = ~2.6 m^2/year. A clay sample with a uniform strength profile was prepared by consolidating a thoroughly mixed, and then de-aired, kaolin slurry at 1 g in a strongbox under a final pressure of 90 kPa. A 30 mm thick medium dense sand layer was then deposited on top of the lower clay layer by raining the sand in water (i.e. through wet pluviation) from a drop height of about 100 mm. The total depth of the sample was about 230 mm (3.83D) above the bottom drainage geofabric-sand layer. The tip of the spudcans penetrated up to ~80 mm (1.33D) and hence the bottom boundary of the strongbox was about 150 mm (2.5D) away from the spudcan. This is well above the critical distance to avoid the bottom boundary influence. The critical distance was suggested as ~0.71~1D (Mandel & Salencon [16]; Meyerhof & Hanna [17]; Ullah et al. [18]).

Soil strength determination

The prepared sand layer produced an average relative density I_D of 60% (effective unit weight of top layer, γ'_t = 9.5 kN/m^3). For the underlying clay bed, characterisation tests were carried out using a T-bar penetrometer of 5 mm in diameter and 20 mm in length. These tests were performed prior to placing the sand layer to avoid the influence of the sand layer trapped at the base of the advancing penetrometer (Lee et al. [19]). A typical shear strength profile is plotted in Figure 2, based on a T-bar factor of $N_{T\text{-}bar}$ =10.5, where z is the penetration depth of the penetrometer mid-diameter in the clay layer. The result in the bottom clay layer gives an averaged undrained shear strength of s_{ub} = 9.3 kPa (7.4~11.1 kPa; effective unit weight of bottom layer, γ'_b = 7 kN/m^3). These properties are also summarised in Table 1.

The tests were carried out using a velocity-controlled system. The T-bar and spudcans were penetrated at a rate of 1 mm/s and 0.2 mm/s, respectively, chosen to balance rate effects against ensuring undrained behaviour in the clay. The normalised velocity index during penetration, $V = vD/c_v$ (where v is the penetration rate) = ~140 > 30, which was expected to be sufficient to ensure undrained conditions in the clay according to Chung et al. [20] and Low et al. [21]. The spudcan penetration rate ensured drained behaviour (with $V < 0.1$) in sand.

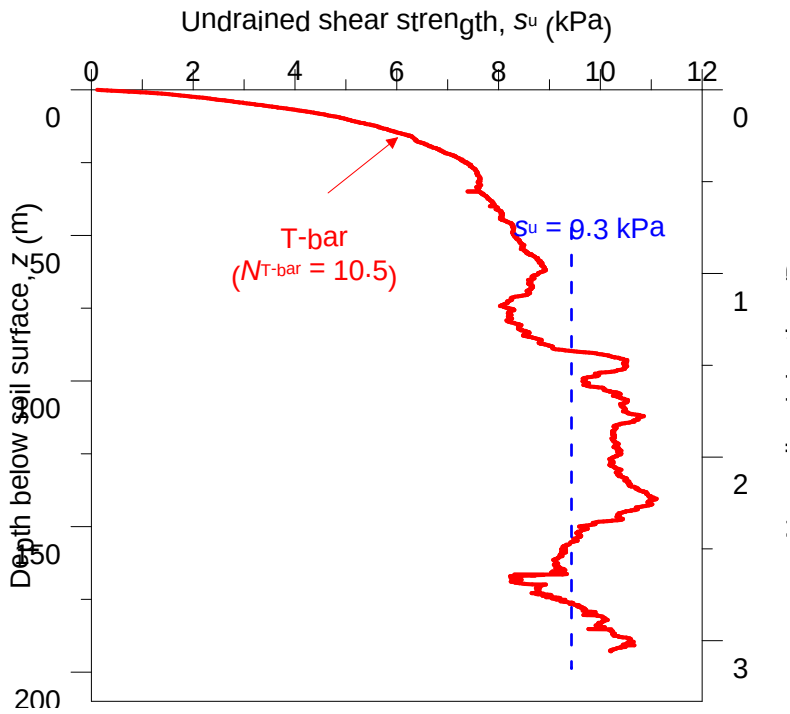

FIGURE 2. Typical shear strength profile of clay layer from T-bar test

TABLE 1. Summary of 1g tests conducted

Spudcan	A	S	H
Test	A1 ~ A3	S1	H1 ~ H2
Geometry	Conventional spudcan	Spudcan with a skirt and 4 slots	Spudcan with 6 holes
Diameter (model), D (mm)	60	60	60
Spudcan base area, A (mm^2)	2827.43	2827.43	2827.43
Spudcan net base area, A_{net} (mm^2)	2827.43	2194.09	2492.55
Spudcan base area reduction ratio $= \frac{A - A_{net}}{A}$ (%)	0	22.40	11.84
Sand thickness, t (mm)	30		
Sand relative density, I_D (%)	60		
Sand effective unit weight, γ'_t (kN/m^3)	9.5		
Clay undrained shear strength, s_{ub} (kPa)	9.3		
Clay effective unit weight, γ'_b (kN/m^3)	7		
Critical depth of punch-through, $h_{P\text{-}T}/D$	0.16, 0.16, 0.12	0.00	0.00
Peak bearing capacity at punch-through, Q_{vp} (N)	88.80, 85.31, 80.36	80.42	88.8, 104.64
Mitigation of punch-through gradient of post-peak bearing capacity reduction, λ	-18.37, -21.15, -7.42	5.66	14.49, 10.38
Reduction of peak bearing capacity (%)	-	5.7	-4.1, -22.6*

* -ve indicates increase in peak bearing capacity

Performance of novel spudcans in mitigating punch-through

The results are presented in terms of penetration resistance, Q_v, as a function of penetration depth of spudcan base, d. Figure 3 shows the results from all penetration tests (A1~A3, S1, H1, H2; Table 1). For the conventional spudcan, punch-through failure was profound for all tests (A1~A3). In the sand layer, the resistance profiles showed a local peak with a subsequent rapid drop. Both spudcan S and spudcan H have eliminated the punch-through risks identified with the conventional spudcan. There was no local peak found, rather the resistance profiles more or less increased with depth. For spudcan S (S1), the capacity in the top sand layer (at the depth of the peak resistance for spudcan A) and in the bottom clay layer were lower than those for spudcan A (see Table 1). This was due to the reduction of the thickness of the effective sand layer beneath the advancing spudcan by the skirt, and critically, as some soils flew through the slots (see the evidence in Figure 4). For spudcan H (H1 and H2), the resistance profiles for full penetration depths were higher than those for spudcan A. The spudcan base area reduction ratio of spudcan H is lower than that of spudcan S (see Table 1), and the geometry and the location of the openings might have influenced the amount of soil flow through the spudcan base (see Figures 4 and 5). In addition, the openings allowed drainage to the sand surface to occur. The effect of more entrapped top stronger soil underneath the spudcan can be seen in the results of numerical analyses discussed in the next section. More studies are needed to provide insight into the influences of various factors.

The severity of punch-through failure is quantified by two measures: (a) degree of post-peak bearing reduction, λ (= $\Delta[Q_v/(d/D)]/s_{u,avg}$; where $s_{u,avg}$ is the average undrained shear strength over $0.5D$ below the sand-clay interface), and (b) apparent (may be lower the field due to e.g. lowering the hull) depth of punch-through prior to establishing equilibrium, $h_{P\text{-}T}$ (Hossain et al. [14]). The values of λ were calculated using the dashed lines in Figure 3 ($\lambda < 0$ indicates the risk of punch-through failure) and are presented in Table 1. The negative values of λ for spudcan A means unsafe against punch-through failure. However, the values of λ have become positive (i.e. safe, see Figure 3) for spudcan S and spudcan H.

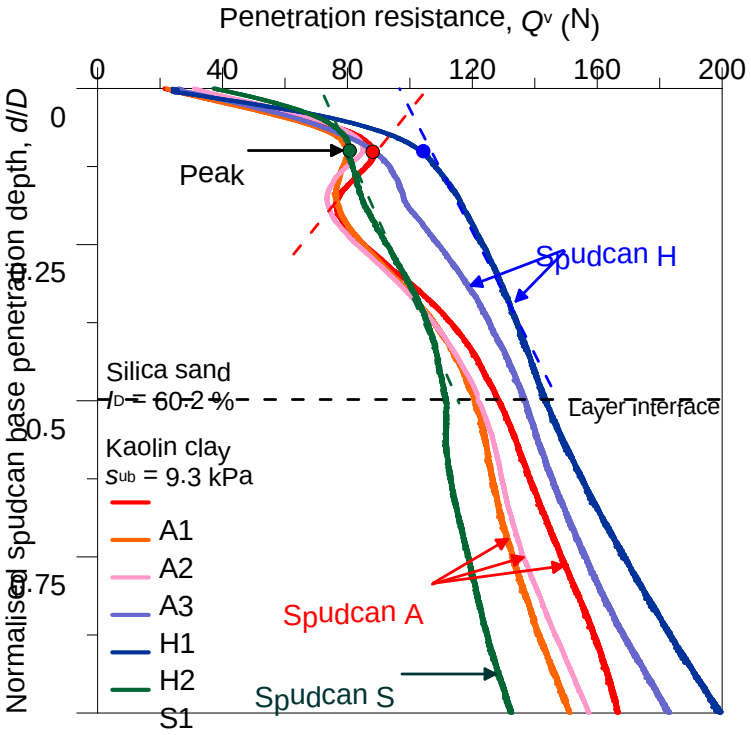

FIGURE 3. Effect of spudcan geometry on penetration resistance profile

FIGURE 4. Evidence of soil flow through slots of spudcan S: (a) Soil column left on extracted spudcan; (b) Soil column on site

FIGURE 5. Evidence of soil flow through holes of spudcan H: (a) Soil column left on extracted spudcan; (b) Soil column on site

NUMERIAL ANALYSIS

Geometry and parameters

This study has considered a circular spudcan of diameter D, penetrating into a two-layer clay deposit, where the top stiff layer with intact uniform undrained shear strength s_{ut}, effective unit weight γ'_t, and thickness t is underlain by the bottom soft layer of non-uniform intact undrained shear strength $s_{ub} = s_{ubs} + k(z - t)$, and effective unit weight γ'_b. s_{ubs} is the intact undrained shear strength of the bottom soft layer at the layer interface. Analyses were undertaken for conventional (spudcan A), 6-hole (spudcan H), and blocked-hole (spudcan H-B) foundations (see Figure 6).

A series of parametric analyses (Groups I~II, Table 2) were performed simulating continuous penetration of spudcan from the seabed surface. The thickness of the top layer, t, was varied relative to the spudcan diameter as $0.35D$~$0.5D$, with nominally infinite thickness of the bottom layer. The strength ratio at the interface between the bottom and top layers, s_{ubs}/s_{ut}, was varied as 0.2~0.25. For convenience, the effective unit weight of the deposit was considered to be constant and was taken as $\gamma' = \gamma'_t = \gamma'_b = 5.88$ kN/m^3. The normalised strength of the bottom layer at the interface was $s_{ubs}/\gamma' D = 0.04, 0.09$, with the degree of non-homogeneity $kD/s_{ubs} = 0, 8$.

CEL method for large deformation problem

3D large deformation finite element (LDFE) analyses were carried out using the Coupled Eulerian-Lagrangian (CEL) approach in the commercial finite element package ABAQUS/Explicit (Dassault Systèmes [22]). The CEL approach is identified as advantageous in circumventing mesh distortion in large deformation problems. The soil is tracked as it flows through an Eulerian mesh, fixed in space, by computing the material volume fraction in each element. The Eulerian element can be materially void or occupied partially or fully by more than one material, with the volume fraction representing the portion of that element filled with a specified material. The structural element, such as a spudcan, is discretised with Lagrangian elements, which can move through the Eulerian mesh without resistance until they encounter Eulerian elements containing soil. The interaction between the structure and the soil is represented using a contact algorithm named 'general contact' in ABAQUS (Dassault Systèmes [22]).

Analysis details

Considering the symmetry of the problem, only a quarter spudcan and soil were modelled. The soil domain was chosen as 4*D* in horizontal and 7*D* in depth, which was testified as sufficiently large to avoid boundary effect. Similar domain sizes were considered by Qiu & Henke [23], Tho et al. [24], Zheng et al. [25, 26] and Hu et al. [27] in spudcan continuous penetration analysis. A typical mesh is shown in Figure 7. The mesh comprised 8-noded linear brick elements with reduced integration, and a fine mesh zone was generated to accommodate the spudcan trajectory during the entire penetration. A 5 m thick void (i.e. material free) layer was set above the soil surface, allowing the soil to heave by flowing into the empty Eulerian elements during the penetration process. The spudcan was simplified as a rigid body and assumed to remain vertical during the penetration process, with no tilt. The penetration velocity of the spudcan was taken as 0.1 m/s.

The soil was modelled as a linear elastic–perfectly plastic material obeying a Tresca yield criterion, but extended as described later to capture strain-rate and strain-softening effects. A uniform stiffness ratio of E/s_{uc} = 200 (where E is the Young's modulus and s_{uc} is the current undrained shear strength after softening and rate effect) was taken throughout the clay profile. All the analyses simulated undrained conditions and adopted a Poisson ratio ν = 0.49 and friction and dilation angles $\phi = \psi = 0$ in total stress analysis. The geostatic stress conditions were modelled using $K_0 = 1$, as the stable penetration resistance (once backflow is fully established) has been found to be unaffected by the value of K_0 (Zhou & Randolph [28]).

Following Einav & Randolph [29], the Tresca soil model was extended in order to take the combined effects of rate dependency and gradual softening into account. The undrained shear strength at individual Gauss points was modified at the beginning of each time step, according to the average rate of maximum shear strain in the previous increments and the current accumulated absolute plastic shear strain, expressed as

$$s_{uc} = \left[1 + \mu \log\left(\frac{\mathrm{Max}\left(|\dot{\gamma}|, \dot{\gamma}_{ref}\right)}{\dot{\gamma}_{ref}}\right)\right]\left[\delta_{rem} + \left(1 - \delta_{rem}\right)e^{-3\xi/\xi_{95}}\right]s_u \quad (1)$$

The first bracketed term augments the strength according to the maximum strain rate, $\dot{\gamma}$ relative to a reference value, $\dot{\gamma}_{ref}$, which was considered as 1.5%/h as consistent with triaxial tests (Lunne et al. [30]), following a logarithmic law with rate parameter μ taken as 0.1 for 'circular' spudcan foundations (Low et al., [21]). The second part of Equation 1 models the degradation of strength according to an exponential function of cumulative shear strain, ξ, from the intact condition to a fully remoulded ratio, δ_{rem} (= $1/S_t = \alpha$). The relative ductility is controlled by the parameter, ξ_{95}, which represents the cumulative shear strain required for 95% remoulding. A typical value of ξ_{95} = 15 (i.e. 1500% shear strain; Randolph, [31]) was considered. Further details can be found in Hossain & Randolph [32] and Zheng et al. [25, 26].

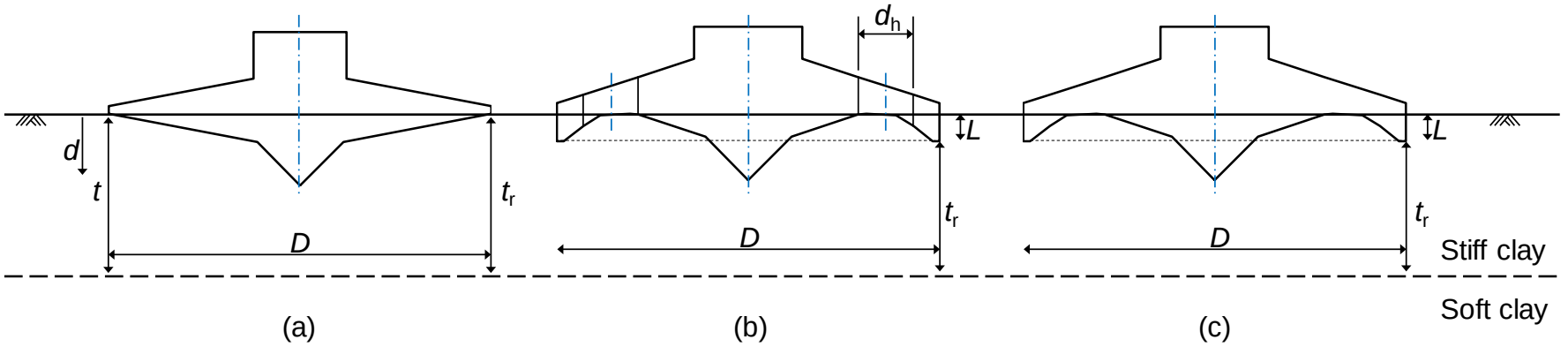

FIGURE 6. Schematic diagram of spudcan shapes (D = 20 m): (a) Conventional (spudcan A); (b) 6-hole (spudcan H); (c) Blocked 6-hole (spudcan H-B)

TABLE 2. Summary of LDFE analyses performed

Test group	Spudcan shape	Spudcan diameter, D (m)	Stiff layer thickness, t (m)	Stiff clay undrained shear strength, s_{ut} (kPa)	Soft clay undrained shear strength, s_{ub} (kPa)	Clay effective unit weight, γ' (kN/m^3)	Apparent punch-through distance, $h_{P\text{-}T}/D$	Peak bearing capacity at punch-through, Q_{vp} (MN)	Mitigation of punch-through gradient of post-peak bearing capacity reduction, λ	Reduction of peak bearing capacity (%)
Group I	A	20	7	50	10	5.88	>1.53	67.46	-1.25	-
	H						1.09	62.90	-0.63	6.76
	H-B						0.79	62.53	-0.50	7.31
Group II	A		10	100	25 + 2(z - t)		>0.46	173.52	-1.632	-
	H						0.00	172.77	0.61	0.43
	H-B						0.00	181.21	1.54	-4.43

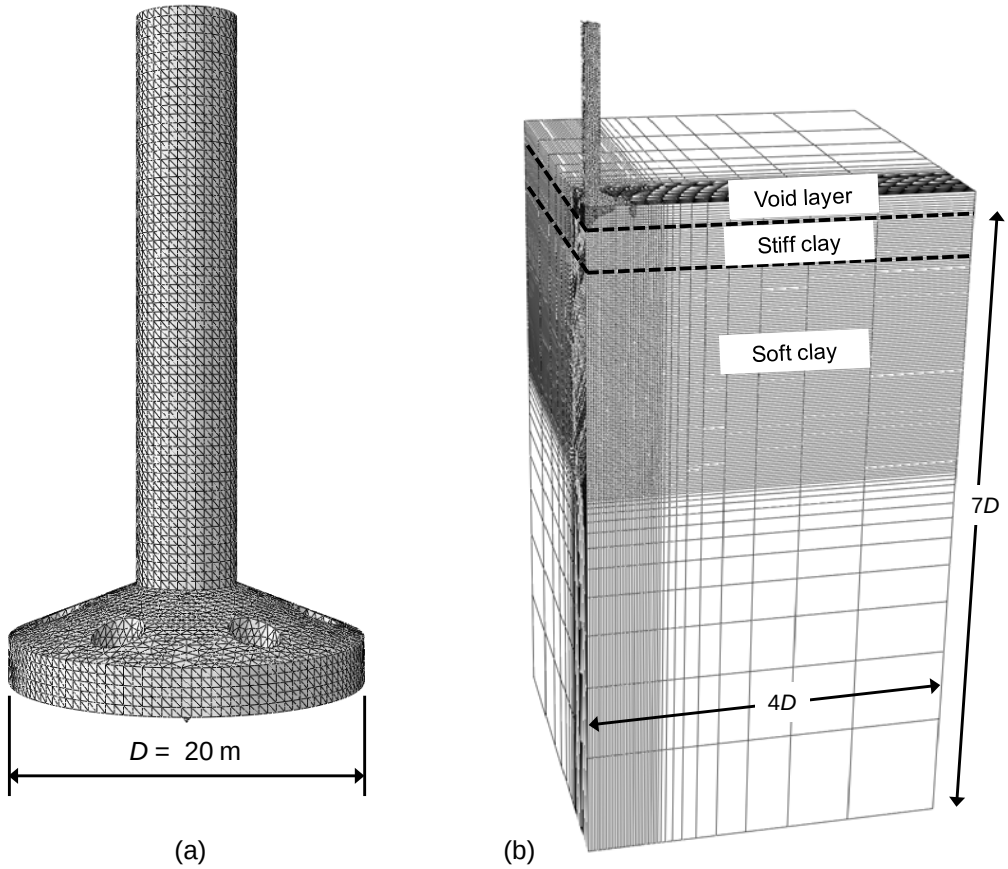

FIGURE 7. Typical mesh used in CEL analysis: (a) Spudcan; (b) Quarter spudcan and soil domain

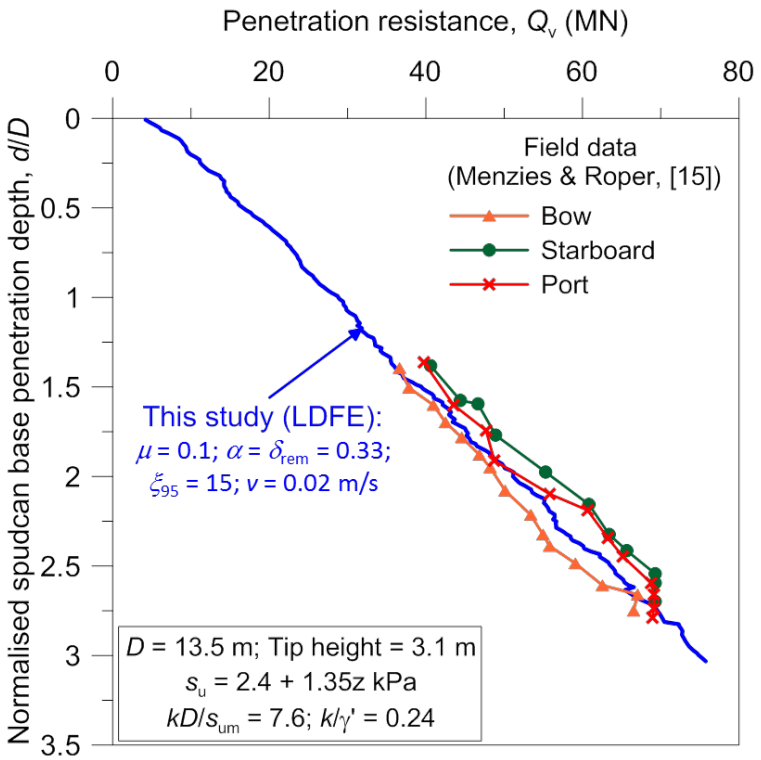

FIGURE 8. Comparison between LDFE result and field data

Validation against field data

A validation exercise was carried out against a case history in the Gulf of Mexico (Site 1, Menzies & Roper [15]). The spudcan foundations were 13.5 m in diameter. The site consisted of normally consolidated clay (sensitivity S_t = ~3) with strength increase linearly with depth as s_u = 2.4 + 1.35z kPa (kD/s_{um} = 7.6, k/γ' = 0.24). An analysis was carried out using these parameters and δ_{rem} = 0.33, μ = 0.1 and ξ_{95} = 15, $\dot{\gamma}_{ref}$ = 1.5%/h. Figure 8 shows penetration resistance profiles as a function of base penetration depth d. The LDFE result is in good agreement with the field data. This validation analysis has confirmed the capability and accuracy of the CEL approach in assessing the penetration resistance during penetration of spudcans in non-homogeneous clay. For parametric analyses, as tabulated in Table 2, parameters in terms of rate dependency and strain-softening were taken as δ_{rem} = 0.33, μ = 0.1 and ξ_{95} = 15, $\dot{\gamma}_{ref}$ = 1.5%/h as they provided good match with the field data.

Performance of novel spudcans in mitigating punch-through

Figures 9 and 10 show sets of penetration resistance profiles of spudcan A, H and H-B for each individual soil profile. For spudcan A, punch-through occurs in the bottom layer for both soil profiles (Group I and II; Table 2). Spudcan H and spudcan H-B either ease (Group I) or eliminate (Group II) the punch-through risks. The values of λ (with $s_{u,avg}$ is now taken as the average undrained shear strength over 0.5D below the peak capacity in the bottom clay layer) were calculated using the dashed lines in Figures 9 and 10 and are presented in Table 2. The negative values of λ, unsafe, for spudcan A have turned to be positive, safe (Figure 10), or mitigated to the less negative values of λ (Figure 9) by spudcan H and spudcan H-B. The performance of spudcan H and spudcan H-B is similar for Group I strength profile whilst that of spudcan H-B is better for Group II strength profile.

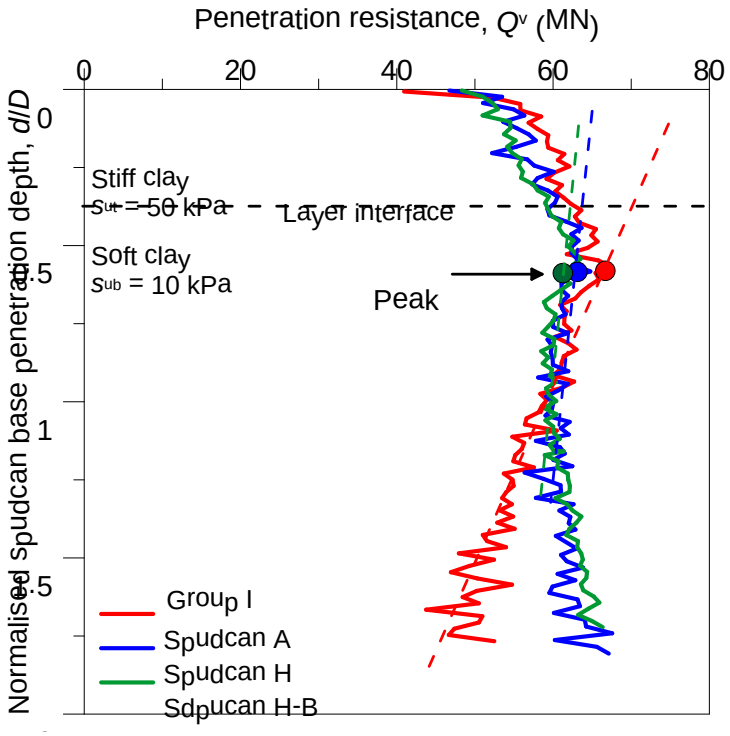

FIGURE 9. Resistance profiles from spudcan A, spudcan H and spudcan H-B penetration (Group I,Table 2)

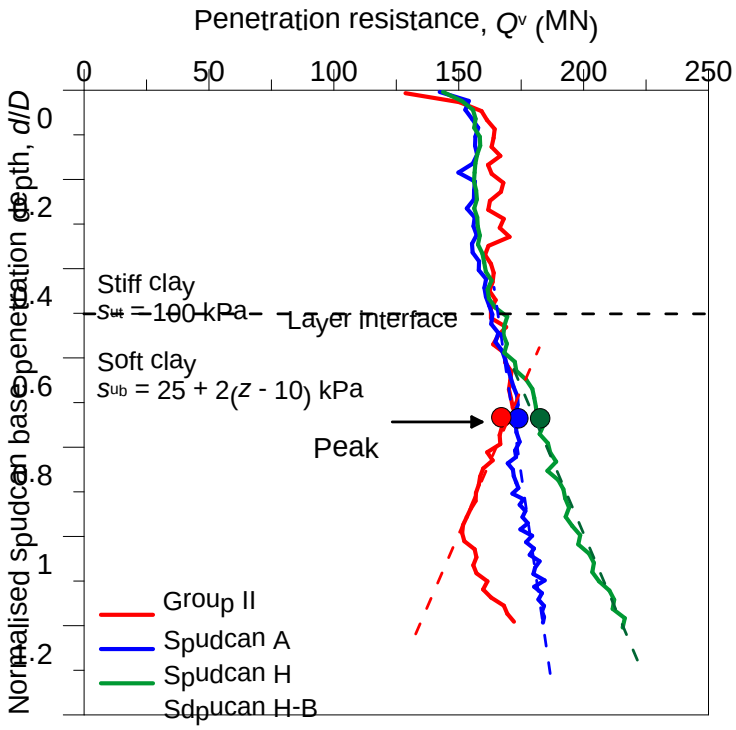

FIGURE 10. Resistance profiles from spudcan A, spudcan H and spudcan H-B penetration (Group II, Table 2)

To provide further explanations, corresponding strength contour at different stages of penetration are illustrated in Figures 11 and 12. For Group I (t/D = 0.35, s_{ubs}/s_{ut} = 0.2, kD/s_{ubs} = 0; Figures 9 and 11), soil plug trapped at the base of spudcans are similar in the top layer, resulting in consistent penetration resistance. At d/D = 0.78 in the bottom layer, the trapped plug starts to breakdown largely by the soil backflow around the spudcan shoulder. This is significant for spudcan A with sloped bottom profile (Figure 6a), leading to a punch-through i.e. sudden reduction in penetration resistance profile. For spudcan H and H-B, a small skirt around the periphery and multi-directional slopes (see Figures 1c, 6b and 6c) allow for restricting a soil plug being trapped at the base. However, small soil flow through the holes of the spudcan with backfilled top results in a smaller soil plug beneath spudcan H compared to spudcan H-B. The height of the trapped soil plug contributes to mobilised penetration resistance in two ways: (a) additional frictional resistance mobilises around the periphery of the plug; (b) the base for mobilising end bearing shifts from the spudcan base to the plug base as the plug acts as if part of the foundation. This is why, in the bottom layer, a significant reduction in penetration resistance occurs for spudcan A, and the profiles rises after a minimal reduction for spudcan H and spudcan H-B.

The doubled shear strength (100 kPa vs 50 kPa) and greater thickness of the top layer for Group II ($s_{ut}/\gamma D$ = 0.85 vs 0.43; t/D = 0.5 vs 0.35) leads to a greater cavity depth above the penetrating spudcan (Figure 12). The cavity allows more soil to flow through the holes of spudcan H, and hence faster breaking of the trapped soil plug relative to spudcan H-B. In summary, both novel spudcans show potential for mitigating or lessening punch-through severity. For stiff-over-soft clay where punch-through occurs in the bottom layer, spudcan H-B, or just a skirted spudcan, shows better performance in this regards.

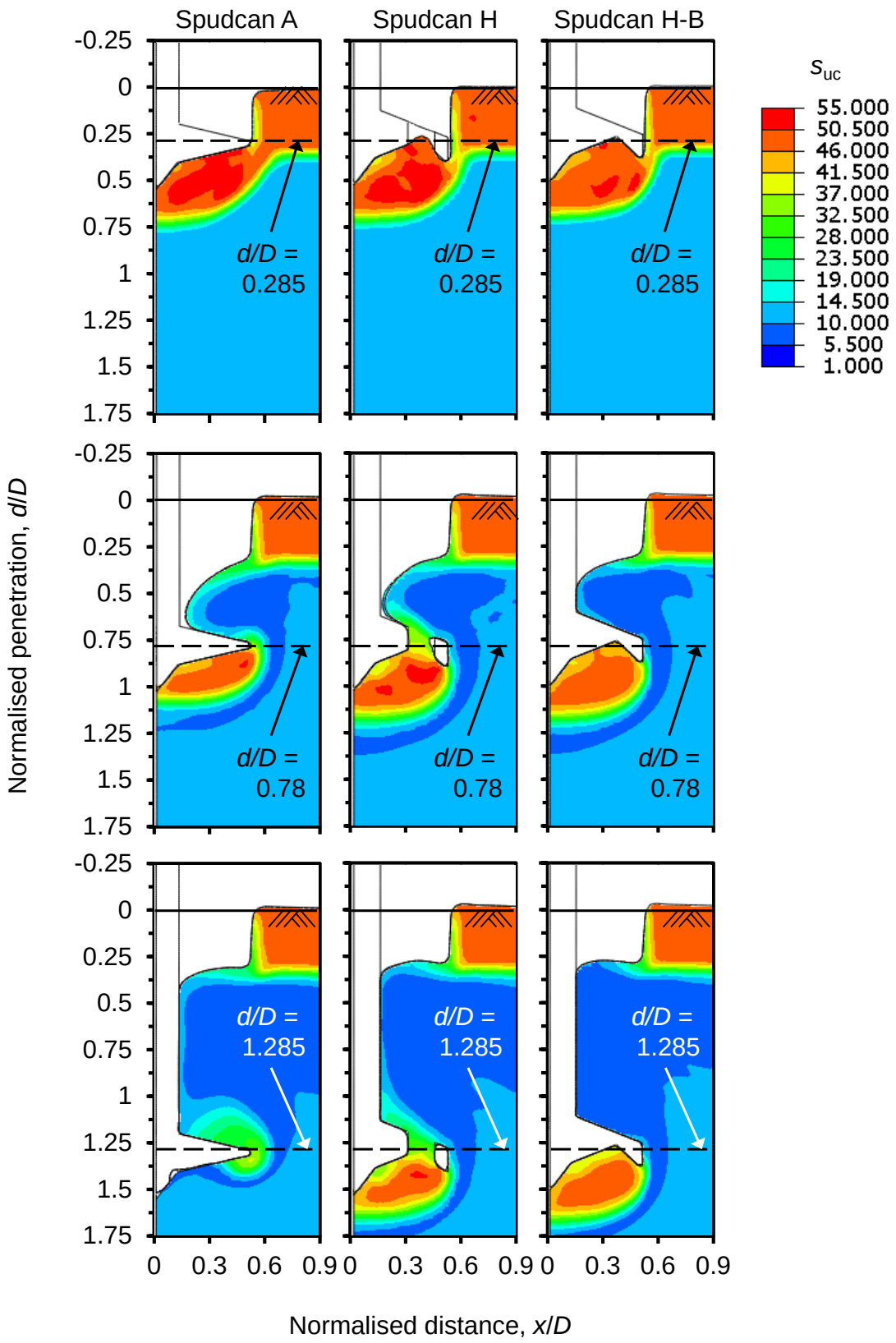

FIGURE 11. Deformed stiff-over-soft clay layers from LDFE simulations at different depths (Group I, Table 2)

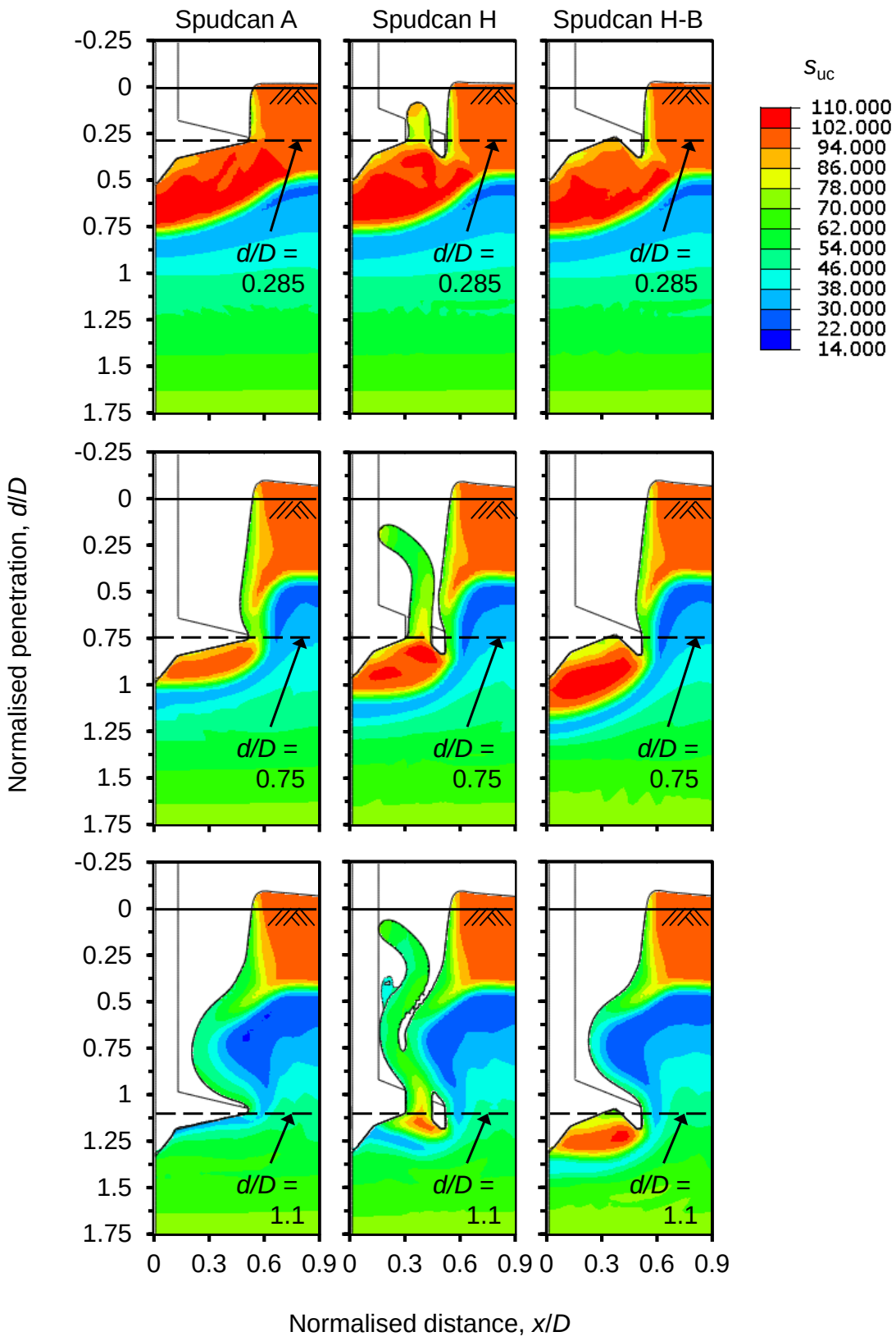

FIGURE 12. Deformed stiff-over-soft clay layers from LDFE simulations at different depths (Group II, Table 2)

CONCLUSIONS

The experimental and numerical results presented in this paper have showed that novel spudcans with skirt and holes are indeed an effective measure at mitigating the risk of punch-through failure when compared against the conventional spudcan without skirt and holes. For the conventional spudcan, punch-through failure was observed during penetration in both sand-over-clay (punch-through occurred in the top layer) and stiff-over-soft clay (punch-through occurred in the bottom layer) deposits. The severity of punch-through failure was quantified by the degree of post-peak bearing reduction (λ). The negative values of λunsafe, for the conventional spudcan somewhat turned to be positive safe or mitigated to the less negative values of λ by the novel spudcans. The amount of stronger soil trapped underneath the spudcan in the bottom soft layer was shown to have a significant effect on punch-through failure mitigations. It seems that the shape and location of the openings in the novel spudcans can be optimised in this regards.

Although the results from LDFE analyses using the CEL approach in ABAQUS was validated against field data in single layer clay, the accuracy is required to be tested against centrifuge test data and numerical results using the RITSS (remeshing and interpolation technique with small strain) approach in ABAQUS.

The results presented in this paper are from a very preliminary study – just to introduce the novel spudcans. More extensive investigations are being carried out through centrifuge model tests, with the objective to (i) provide further scientific insight, to (ii) quantify the influence of the novel spudcan geometry on vertical-horizontal-moment capacity envelope and uplift resistance, and to (iii) develop design guidelines for use by industry.

ACKNOWLEDGEMENTS

The research presented herein was undertaken with support from the Australian Research Council (ARC) through the Linkage Project LP140100066. The third author is an ARC Discovery Early Career Researcher Award (DECRA) Fellow and is supported by the ARC Project DE140100903. The work forms part of the activities of the Centre for Offshore Foundation Systems (COFS), currently supported as a node of the Australian Research Council Centre of Excellence for Geotechnical Science and Engineering and as a Centre of Excellence by the Lloyd's Register Foundation. This support is gratefully acknowledged, as is the assistance of the technicians, Mr. Manuel Palacios and Mr. Kelvin Leong.

NOTATION

A	spudcan base area
A_{net}	spudcan net base area
c_v	consolidation coefficient
D	diameter of spudcan at largest section or outer diameter of skirted foundation
d	penetration depth at largest section of spudcan
d_h	diameter of hole on spudcan
d_{50}	average particle size
E	Young's modulus
e_{max}	maximum void ratio
e_{min}	minimum void ratio
G_s	specific gravity
$h_{P\text{-}T}$	apparent punch-through distance
I_D	average relative density of sand
I_p	plasticity index
K_0	coefficient of earth pressure at the rest
k	shear strength gradient with depth
L	length of skirt
LL	liquid limit
$N_{T\text{-}bar}$	bearing factor of T-bar penetrometer

Q_v penetration resistance
Q_{vp} peak bearing capacity at punch-through
S_t soil sensitivity
s_u intact undrained shear strength
s_{ub} intact undrained shear strength in bottom layer
s_{ubs} intact undrained shear strength of bottom layer at layer interface
s_{uc} current undrained shear strength after softening and rate effect
s_{um} intact undrained shear strength at mudline
s_{ut} intact undrained shear strength in top layer
$s_{u,avg}$ intact undrained shear strength averaged over $0.5D$ below the interface (for punch-through in top layer) or below depth of punch-through (for punch-through in bottom layer)
t thickness of top layer
t_r thickness of sand layer beneath spudcan base or skirt tip
V normalised velocity index
v velocity of object (spudcan or T-bar or piezocne)
x distance from center of spudcan
z depth below soil surface
α interface friction ratio
δ_{rem} remoulded strength ratio
ϕ friction angle
ϕ_{cv} critical state friction angle
$\dot{\gamma}$ shear strain rate
$\dot{\gamma}_{ref}$ reference shear strain rate
γ' effective unit weight of soil
γ'_b effective unit weight of bottom layer soil
γ'_t effective unit weight of top layer soil
λ gradient of post-peak bearing capacity reduction
μ rate parameter for logarithmic model
ν Poisson's ratio
ψ dilation angle
ξ cumulative plastic shear strain
ξ_{95} cumulative plastic shear strain required for 95% remoulding

REFERENCES

[1] ISO (International Organization for Standardization). Petroleum and natural gas industries – site specific assessment of mobile offshore units – part 1: jack-ups, ISO 19905-1. Geneva: ISO, 2012.

[2] InSafeJIP(Joint Industry Funded Project). Improved guidelines for the prediction of geotechnical performance of spudcan foundations during installation and removal of jack-up units. Surrey: RPS Energy, 2010.

[3] Aust T, editor. Accident to the mobile offshore drilling unit Maersk Victory on 16 november 1996. South Australia: Mines and Energy Resources, 1997.

[4] Kostelnik A, Guerra M, Alford J, Vazquez J, Zhong, J- Jackup mobilization in hazardous soils, SPE Drilling and Completion. 2007:22(1):4-15.

[5] SNAME(Society of Naval Architects and Marine Engineers). Guidelines for site specific assessment of mobile jack-up units, technical and research bulletin 5-5A, 1st edition – rev. 3. 2008.

[6] Jack RL, Hoyle MJR, Hunt RJ, Smith NP- Jack-up accident statistics: lots to learn. In: Proceedings, Eleventh International Conference: The Jack-up Platform Design, Construction and Operation. London, 2007.

[7] Jack RL, Hoyle MJR, Smith NP, Hunt RJ- Jack-up accident statistics – a further update. In: Proceedings, Fourteenth International Conference on the Jack-up Platform Design, Construction and Operation. London, 2013.
[8] Erbrich CT- Australian frontiers – spudcans on the edge. In: Proceedings, The International Symposium on Frontiers in Offshore Geotechnics (ISFOG 2005). Perth, 2005. p 49–74.
[9] Brennan R, Diana H, Stonor RWP, Hoyle MJR, Cheng CP, Martin D, Roper R- Installing jackups in punch-through-sensitive clays. In: Proceedings, Offshore Technology Conference. Houston, 2006. OTC 18268.
[10] Hossain MS, Cassidy MJ, Daley D, Hannan R- Experimental investigation of perforation drilling in stiff-over-soft clay, Applied Ocean Research. 2010:32(1):113-123.
[11] Hossain MS, Cassidy MJ, Baker R, Randolph MF- Optimisation of perforation drilling for mitigating punch-through in multi-layered clays, Canadian Geotechnical Journal. 2011:48(11):1658-1673.
[12] Svanø G, Tjelta TI- Skirted spudcans – extending operational depth and improving performance, Marine Structures. 1996:9(1):129-148.
[13] Gan CT, Teh KL, Leung CF, Chow YK, Swee S- Behaviour of skirted footings on sand overlying clay. In: Proceedings, Second International Symposium on Frontiers in Offshore Geotechnics, ISFOG. Perth, 2011. p 415-420.
[14] Hossain MS, Zheng J, Menzies D, Meyer L, Randolph MF- Spudcan penetration analysis for case histories in clay, Journal of Geotechnical and Geoenvironmental Engineering. 2014:140(7):04014034.
[15] Menzies D, Roper R- Comparison of jackup rig spudcan penetration methods in clay. In: Proceedings, Offshore Technology Conference. Houston, 2008. OTC 19545.
[16] Mandel J, Salencon J- The bearing capacity of soils on a rock foundation. In: Proceedings, Seventh International Conference on Soil Mechanics and Foundation Engineering. Mexico City: Sociedad Mexicana de Mecanica,1969. p 157-164.
[17] Meyerhof GG, Hanna AM- Ultimate bearing capacity of foundations on layered soils under inclined load, Canadian Geotechnical Journal. 1978:15(4):565-572.
[18] Ullah SN, Hu Y, White D, Stanier S- LDFE study of bottom boundary effect in foundation model tests, International Journal of Physical Modelling in Geotechnics. 2014:14(3):80–87.
[19] Lee KK, Cassidy MJ, Randolph MF- Bearing capacity on sand overlying clay soils: experimental and finite element investigation of potential punch-through failure, Géotechnique. 2013:63(15):1271-1284.
[20] Chung SF, Randolph MF, Schneider JA- Effect of penetration rate on penetrometer resistance in clay, Journal of Geotechnical and Geoenvironmental Engineering. 2006:132(9):1188-1196.
[21] Low HE, Randolph MF, DeJong JT, Yafrate NJ- Variable rate full-flow penetration tests in intact and remoulded soil. In: Proceedings, Third International Conference on Geotechnical and Geophysical Site Characterization, Taylor & Francis Group. Taipei, 2008. p 1087-1092.
[22] Dassault Systèmes. Abaqus 6.11 online documentation. Providence: Dassault Systèmes Simula Corp, 2011.
[23] Qiu G, Henke S- Controlled installation of spudcan foundations on loose sand overlying weak clay, Marine Structure. 2011:24(4):528-550.
[24] Tho KK, Leung CF, Chow YK, Swaddiwudhipong S- Eulerian finite-element technique for analysis of jack-up spudcan penetration, International Journal of Geomechanics. 2012:12(1):64-73.
[25] Zheng J, Hossain M, Wang D- Numerical modeling of spudcan deep penetration in three-layer clays, International Journal of Geomechanics. 2014:10.1061/(ASCE)GM.1943-5622.0000439.
[26] Zheng J, Hossain M, Wang D- New design approach for spudcan penetration in nonuniform clay with an interbedded stiff layer, Journal of Geotechnical and Geoenvironmental Engineering. 2015:141(4):04015003.
[27] Hu P, Wang D, Stanier SA, Cassidy MJ- Assessing the punch-through hazard of a spudcan on sand overlying clay, Géotechnique, DOI: 10.1680/geot.14.P.097.
[28] Zhou H, Randolph MF- Resistance of full-flow penetrometers in rate-dependent and strain-softening clay, Géotechnique. 2009:59(2):79-86.
[29] Einav I, Randolph M- Combining upper bound and strain path methods for evaluating penetration resistance, International Journal for Numerical Methods in Engineering. 2005:63(14):1991-2016.

[30] Lunne T, Berre T, Andersen KH, Strandvik S, Sjursen M- Effects of sample disturbance and consolidation procedures on measured shear strength of soft marine Norwegian clays, Canadian Geotechnical Journal. 2006:43(7):726–750.
[31] Randolph MF- Characterisation of soft sediments for offshore applications. Keynote lecture. In: Proceedings, Second International Conference on Site Characterisation. Porto, 2004. p 209–231.
[32] Hossain MS, Randolph MF New mechanism-based design approach for spudcan foundations on stiff-over-soft clay. In: Proceedings, Offshore Technology Conference. Houston, 2009. OTC 19907.